

## PDF hosted at the Radboud Repository of the Radboud University Nijmegen

The following full text is a publisher's version.

For additional information about this publication click this link.

<http://hdl.handle.net/2066/28854>

Please be advised that this information was generated on 2017-12-05 and may be subject to change.



## EFFECT OF LINEAR POLARISABILITY AND LOCAL FIELDS ON SURFACE SHG

C.M.J. Wijers, P.L. de Boeij

*Faculty of Applied Physics, University of Twente, P.O. Box 217,  
NL 7500 AE Enschede, The Netherlands*

C.W. van Hasselt, Th. Rasing

*Research Institute for Materials, University of Nijmegen, Toernooiveld,  
NL 6525 ED Nijmegen, The Netherlands*

(Received June 9, 1994 by G. Güntherodt)

(accepted for publication 11 September 1994 by G. Güntherodt)

A discrete dipole model has been developed to describe Surface Second Harmonic Generation by centrosymmetric semiconductors. The double cell method, which enables the linear reflection problem to be solved numerically for semi-infinite systems, has been extended for the nonlinear case. It is shown that a single layer of nonlinear electric dipoles at the surface and nonlocal effects allows to describe the angle of incidence dependent anisotropic SHG obtained from oxidised Si(001) wafers. The influence of the linear response, turns out to be essential to understand the anisotropic SHG-process.

Keywords: A. surface and interfaces, D. optical properties, E. nonlinear optics

In recent years Surface Second Harmonic Generation (SSHG) has become a widely used surface and interface probe. Its sensitivity to the symmetry of crystalline surfaces has been particularly successful<sup>1-4</sup>. To describe SSHG, commonly use is made of macroscopic continuum models, with a strong emphasis on symmetry arguments<sup>5,6</sup>. Purely microscopic models have as yet not been capable to treat SSHG, although a few authors have used partially microscopic models<sup>7,8</sup> in order to take into account local field effects.

In this paper we show the first results of an alternative approach to describe SSHG, the nonlinear discrete dipole model. This model is strictly microscopic and goes as such beyond what macroscopic continuum models can treat. It yields the microscopic sources and microscopic electric fields in the surface region, both for the fundamental and second harmonic frequency. Nonlocal electrodynamic interactions, including retardation, are rigorously taken into account and demonstrate how local fields play a role in the SSHG process. The nonlinear behaviour of the discrete dipole theory was already studied by us for thin slabs<sup>9</sup>, but the configuration relevant for experiment, is the semi-infinite one.

By means of the linear double cell method the local electric fields can be obtained for arbitrary semi-infinite crystalline systems<sup>10,11</sup>. This method requires the system, represented by lattice planes of dipoles, to be subdivided into a semi-infinite bulk region and a (thin) surface region on top of it. The response of the bulk region is governed by a finite number of normal modes. The double cell method makes the coupling between the surface and

the bulk regions using those normal modes. Off-normal incidence cases benefit particularly of the incorporation of retardation.

In this paper we give the nonlinear extension of the double cell method, which enables the description of the angle of incidence dependence and the rotational anisotropy of SHG for semi-infinite crystals. To demonstrate the potential abilities of such an approach, we will apply the method to the Si(001) surface, and make a comparison with experiment. The crystal and surface symmetry, as revealed by the anisotropy of the nonlinear response, is taken into account in the present analysis. We will also investigate the relative contributions of surface and bulk to SHG.

The crystal and its surface are represented by a corresponding semi-infinite crystalline lattice of point-like dipoles, which are induced by the local electric fields. Each lattice plane is spanned by the lateral basis vectors  $\mathbf{s}_1$  and  $\mathbf{s}_2$ . The  $z$ -direction is normal to the surface, pointing to the crystal interior. Parallel translational symmetry requires that all dipoles within a lattice plane  $i$  parallel to the surface are equivalent, and can be represented by a single characteristic dipole  $\mathbf{p}_i$ , positioned at  $\mathbf{r}_i$ . The local fields are superpositions of the externally applied electric field and the electric fields produced by all dipole sources in the system. The incident light has an electric field given by the real part of

$$\mathbf{E}_{ext}(\mathbf{r}, t) = E_0 \hat{\mathbf{e}} \exp(i[\mathbf{k}\mathbf{r} - \omega t]), \quad (1)$$

where  $E_0$  is the amplitude and  $\hat{\mathbf{e}}$  the direction of po-

larisation. The wave vector is  $\mathbf{k}$  and the frequency  $\omega$ . The fields produced by the dipoles are obtained through the transfer-tensors  $f_{ij}$  which are derived from the microscopic Maxwell equations (SI-units). Techniques to calculate them efficiently can be found in<sup>10,11</sup>. The interaction equations for the characteristic dipoles follow from the linear induction principle:

$$\mathbf{p}_i = \vec{\alpha}_i \mathbf{E}_{L,i} = \vec{\alpha}_i (\mathbf{E}_{ext}(\mathbf{r}_i) + \sum_j \vec{f}_{ij} \mathbf{p}_j), \quad (2)$$

where  $\alpha_i$  is the linear polarisability tensor and  $\mathbf{E}_{L,i}$  the local field at  $\mathbf{r}_i$ .

In the double cell method the solution of the collective response of the interacting dipoles to the externally applied field starts by finding the normal modes. They make up the collective oscillations of the bulk region which can be written as:

$$\mathbf{p}_i = \sum_{m=1}^M v_m \mathbf{u}_m \exp(i[\mathbf{k}_{\parallel} + q_m \hat{\mathbf{z}}] \mathbf{r}_i). \quad (3)$$

Here  $v_m$  is the normal mode strength. The normal mode polarisation  $\mathbf{u}_m$  and the (complex) normal mode wave number  $q_m$  are entirely determined by the bulk properties and obey the bulk secular equation<sup>10,11</sup>. For bulk silicon only two normal modes ( $q_m, \mathbf{u}_m$ ) are needed at optical frequencies for each wave vector  $\mathbf{k}$ .

The individual dipole strengths  $\mathbf{p}_i$  of the surface region, and the two normal mode strengths  $v_m$  of the bulk region are the only unknowns left, and they can be found by solving the double cell interaction equations:

$$\begin{pmatrix} \mathcal{M}_{SS} & \mathcal{M}_{SB} \\ \mathcal{M}_{BS} & \mathcal{M}_{BB} \end{pmatrix} \begin{pmatrix} \mathbf{p}_i \\ v_m \end{pmatrix} = \begin{pmatrix} \mathbf{E}_{ext}(\mathbf{r}_i) \\ E_0(\hat{\mathbf{t}} \cdot \hat{\mathbf{e}}) \end{pmatrix}. \quad (4)$$

The sub-matrix  $\mathcal{M}_{SS}$  is a composite matrix of transfer tensors coupling the surface dipoles, and the sub-matrix  $\mathcal{M}_{BB}$  is a simple  $2 \times 2$  complex matrix coupling the two normal modes. The off-diagonal matrices connect the surface and the bulk regions, which shows that for the bulk region only the normal mode strengths  $v_m$  are affected by the surface region. The bulk part of the inhomogeneous vector corresponds to the  $s$ - and  $p$ -components (generically  $\mathbf{t}$ ) of the incoming light. From the microscopic sources the microscopic and macroscopic fields can be obtained. The  $\mathbf{t}$  polarised component of the reflected field  $\mathbf{E}$  is obtained from the superposition of all fields produced by these sources:

$$\mathbf{E}^t = \frac{ik^2/2\epsilon_0}{|\mathbf{s}_1 \times \mathbf{s}_2| |\mathbf{k}_z|} \left[ \sum_{i=1}^{\infty} \hat{\mathbf{t}} \cdot \mathbf{p}_i \exp(-i[\mathbf{k}_{\parallel} - k_z \hat{\mathbf{z}}] \mathbf{r}_i) \right]. \quad (5)$$

The dipole strengths for the bulk region have to be obtained from Eq. (3).

For a linear bulk the extension of the double cell method to the nonlinear optical response can be made without much difficulty. The nonlinear behaviour is restricted to the surface region only, where the induction principle for the dipoles is given by<sup>9</sup>

$$\mathbf{p}_i(2\omega) = \vec{\alpha}_i(2\omega) \mathbf{E}_{L,i}(2\omega) + \vec{\beta}_i(2\omega) \mathbf{E}_{L,i}(\omega) \mathbf{E}_{L,i}(\omega). \quad (6)$$

In the bulk we keep the linear induction principle. As a result all normal modes can be obtained in the usual way<sup>10</sup>. We found by direct calculation that beam depletion can be neglected. Therefore the linear double cell method can be used in an unabridged way to solve for the local fields in the surface region at the fundamental frequency. With these fields at hand, the nonlinear term at the right hand side of Eq. (6) can be calculated. That the same equation will generate all higher harmonics, due to local fields, will be ignored however. The nonlinear sources  $\mathbf{p}_i(2\omega)$  and  $v_m(2\omega)$  can now be obtained by solving the interaction equations for the double frequency, after modifying the inhomogeneous vector by omitting the bulk part and replacing the surface part by<sup>9</sup>:

$$\mathbf{E}_{ext}(\mathbf{r}_i) \rightsquigarrow \vec{\alpha}_i^{-1}(2\omega) \vec{\beta}_i(2\omega) \mathbf{E}_{L,i}(\omega) \mathbf{E}_{L,i}(\omega). \quad (7)$$

With the sources known at both frequencies, the linear and nonlinear reflected fields can be obtained by Eq. (5).

For the dipole model of the unreconstructed Si(001) surface we used a bulk truncated geometry where each dipole represents two atoms<sup>12</sup>. The atomic diamond lattice then corresponds to an fcc dipole lattice, with dipoles positioned at  $(0, 0, 0)$  and  $(\frac{1}{2}a, 0, \frac{1}{2}a)$ , in the elementary cell, and lattice vectors  $\mathbf{s}_1 = (a, 0, 0)$ ,  $\mathbf{s}_2 = (\frac{1}{2}a, \frac{1}{2}a, 0)$  and  $\mathbf{s}_3 = (0, 0, a)$ ,  $a$  is the lattice parameter. The value for the isotropic bulk polarisability is obtained from the dielectric constant using the Clausius-Mossotti relation. We used for the lattice parameter  $a = 5.43\text{\AA}$ , and for the dielectric constant  $\epsilon = 17.2241 + i0.4296$  at  $2.33\text{eV}$  and  $\epsilon = -16.2864 + i16.4968$  at  $4.66\text{eV}$ <sup>13</sup>.

The (001) surface of the implemented dipole configuration has the  $2mm$  symmetry of a bulk truncated diamond lattice, with two mirror planes  $(110)$  and  $(1\bar{1}0)$ . This symmetry is reflected in the (hyper)polarisabilities of the surface dipoles. This restricts the polarisability  $\alpha$  to three independent elements

$$\vec{\alpha} = \alpha_{iso}^{\perp\perp}(\hat{\mathbf{z}}\hat{\mathbf{z}}) + \alpha_{iso}^{\parallel\parallel}(\hat{\mathbf{x}}\hat{\mathbf{x}} + \hat{\mathbf{y}}\hat{\mathbf{y}}) + \alpha_{ani}^{\parallel\parallel}(\hat{\mathbf{x}}\hat{\mathbf{y}} + \hat{\mathbf{y}}\hat{\mathbf{x}}), \quad (8)$$

and the hyper-polarisability tensor  $\beta$  to five<sup>14</sup>

$$\begin{aligned} \vec{\beta} = & \beta_{iso}^{\perp\perp\perp}(\hat{\mathbf{z}}\hat{\mathbf{z}}\hat{\mathbf{z}}) + \beta_{iso}^{\perp\parallel\parallel}(\hat{\mathbf{x}}\hat{\mathbf{x}}\hat{\mathbf{z}} + \hat{\mathbf{x}}\hat{\mathbf{z}}\hat{\mathbf{x}} + \hat{\mathbf{y}}\hat{\mathbf{y}}\hat{\mathbf{z}} + \hat{\mathbf{y}}\hat{\mathbf{z}}\hat{\mathbf{y}}) + \\ & \beta_{iso}^{\perp\parallel\parallel}(\hat{\mathbf{z}}\hat{\mathbf{x}}\hat{\mathbf{x}} + \hat{\mathbf{z}}\hat{\mathbf{y}}\hat{\mathbf{y}}) + \beta_{ani}^{\perp\parallel\parallel}(\hat{\mathbf{z}}\hat{\mathbf{x}}\hat{\mathbf{y}} + \hat{\mathbf{z}}\hat{\mathbf{y}}\hat{\mathbf{x}}) + \\ & \beta_{ani}^{\parallel\perp\perp}(\hat{\mathbf{x}}\hat{\mathbf{y}}\hat{\mathbf{z}} + \hat{\mathbf{x}}\hat{\mathbf{z}}\hat{\mathbf{y}} + \hat{\mathbf{y}}\hat{\mathbf{x}}\hat{\mathbf{z}} + \hat{\mathbf{y}}\hat{\mathbf{z}}\hat{\mathbf{x}}). \end{aligned} \quad (9)$$

The upper indices  $\parallel$  and  $\perp$  refer to the orientation relative to the surface. Isotropic parts are invariant under rotations about the surface normal. The two isotropic elements in  $\alpha$  have bulk values. The hyper-polarisability and the anisotropy in the polarisability are assigned only to the *topmost layer* of dipoles. The rest of the system is bulk-like.

The macroscopic  $4mm$  symmetry observed in experiments is a result of the simultaneous presence of two different domains<sup>2,15</sup>, which have their orientations rotated by  $90^\circ$  about the surface normal. With the  $2mm$  symmetry of the dipole model, the macroscopic  $4mm$  symmetry is restored by the superposition of the coherently reflected fields of both domains. This, however, does not result in the exclusion of the anisotropic elements in  $\alpha$

and  $\beta$ , as is the case for the macroscopic response tensor  $\chi$  used in phenomenological models.

In order to apply this model to an experimental case, we measured the p-polarised anisotropic SHG by Si(001) in air for s- and p-polarised excitation at angles of incidence between  $15^\circ$  and  $75^\circ$ . For the excitation the frequency-doubled output at 532 nm of a seeded Q-switched Nd-YAG laser was used. The fluence of the 8 ns pulses was limited to  $30 \text{ mJ/cm}^2$ , well below the damage threshold, and stable within 2%. The sample was an optically flat standard Si wafer, cut within  $0.5^\circ$  to the (001) axis, and with a thin natural oxide. For the oxidised surface we used a bulk truncated geometry and the oxide will only affect the absolute values of the linear and nonlinear surface polarisabilities.

The discrete dipole calculations performed on this model system gave, in agreement with the macroscopic 4mm symmetry<sup>2,15</sup>, isotropic linear reflection coefficients and anisotropic s- and p-polarised second harmonic fields, which have azimuthal dependences according to:

$$\mathbf{E}_{2\omega}^s(\theta, \Omega) = a_1(\theta) \sin(4\Omega) \quad (10)$$

$$\mathbf{E}_{2\omega}^p(\theta, \Omega) = b_0(\theta) + b_1(\theta) \cos(4\Omega). \quad (11)$$

Here  $\Omega$  is the azimuthal angle between the plane of incidence and the in-plane (100) direction,  $\theta$  is the angle of incidence and the complex numbers  $a_1$ ,  $b_0$  and  $b_1$  are linear combinations of the  $\beta$  tensor elements, depending on the excitation polarisation. Anisotropy is required for both polarizability  $\alpha$  and hyperpolarizability  $\beta$  of the surface layer, to get agreement between theory and experiment. For an isotropic  $\alpha$  already an anisotropy in the SHG signal is obtained, but the value is too weak (4 orders smaller than the isotropic part of the p-polarised signal), to explain the experiments. For a wide range of  $\alpha_{ani}^{\parallel\parallel}$  we can get excellent agreement with experiment by fitting the elements of  $\beta$  to the p-polarised intensities, which can be described by:

$$|\mathbf{E}(2\omega)|^2 = A(\theta) + B(\theta)\cos(4\Omega) + C(\theta)\cos(8\Omega). \quad (12)$$

Here A, B and C are real numbers obtained from Eq (11) with  $A = |b_0|^2 + \frac{1}{2}|b_1|^2$ ,  $B = 2\text{Re}(b_1^*b_0)$  and  $C = \frac{1}{2}|b_1|^2$ .

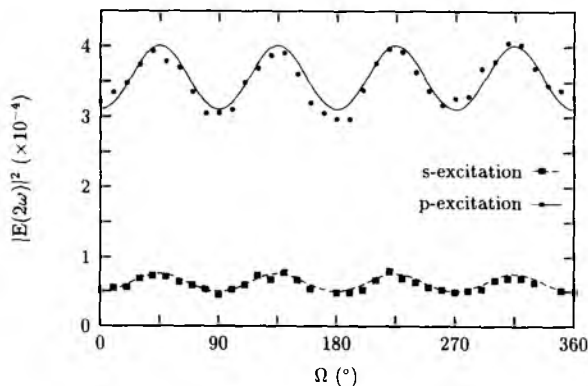


FIG. 1. Azimuthal dependence of the p-polarised SH intensity for Si (100). s/p-polarised excitation, ( $\theta = 45^\circ$ ). Lines: calculation (in units of  $I_2^2$ ), dots: experiment (arb. units)

It has been shown that the anisotropy present on a dimer reconstructed Ge(001) surface was removed by exposure to molecular oxygen, but that also some anisotropy remained if atomic oxygen was used instead<sup>16</sup>. We used  $\alpha_{ani}^{\parallel\parallel} = 1\%$  of the bulk value for both frequencies, which results in an anisotropy of the linear reflection from a single domain of  $3 \times 10^{-6}$ , well below their experimental resolution. Fig. (1) shows the full anisotropy for a  $45^\circ$  angle of incidence.

In Fig. (2) the angle of incidence dependence of the coefficients A and B is shown for p-polarised SHG under s- and p-polarised excitation. The dots are measurements and the curves are results of the theory for the fitted  $\beta$  (listed in table (I) in units of  $\beta_0$ ). A, B and  $|\mathbf{E}(2\omega)|^2$  are given in units of  $I_2^2 = (|\mathbf{E}_0|^2\beta_0/4\pi\epsilon_0a^3)^2$ . All experimental data for s- and p-polarised excitation have the same scaling.

Table (I) shows that a small anisotropy in the linear polarisability of the topmost layer (1%) requires a large anisotropy in the nonlinear coefficients ( $\beta_{ani}/\beta_{iso} \sim 30$ ). For the SHG response, this leads to a strong anisotropic response ( $\sim 10\%$ , see Fig. (2)), whereas this anisotropic linear surface term leads to a fully isotropic linear reflection for a multi-domain sample of 4mm symmetry.

For p-polarised excitation the moduli of the second harmonic dipole strengths (in units of  $\beta_0|E_0|^2$ ) are shown in Fig. (3) as a function of layer index  $i$ . The figure shows also the modulus of this dipole strength, obtained from the normal mode expansion Eq. (3) extrapolated up to the surface, and the modulus of the difference between the two types of vectors. Within our approach this is

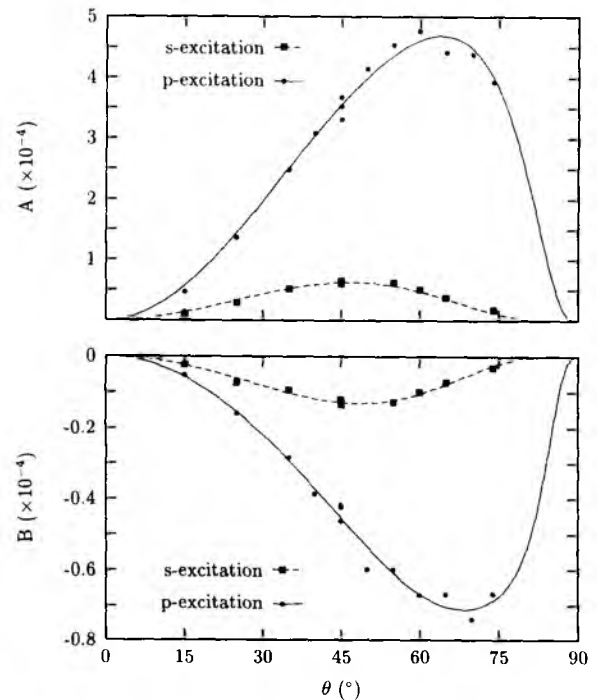


FIG. 2. Coefficients A (isotropic part) and B (anisotropic part) as a function of  $\theta$  for Si(001). s/p-polarised excitation. Lines: calculation (in units of  $I_2^2$ ), dots: experiment (arb. units)

TABLE I. elements of  $\beta$  for  $\alpha_{ani}^{||} = 0.01\alpha_{iso}^{||}$ 

	value ( $\times\beta_0$ )		value ( $\times\beta_0$ )
$\beta_{iso}^{\perp\perp\perp}$	0.2783		
$\beta_{iso}^{\perp  }$	$-0.9940 - i 1.869$	$\beta_{ani}^{\perp  }$	$24.591 + i 45.170$
$\beta_{iso}^{  \perp}$	$-0.6142 - i 0.5516$	$\beta_{ani}^{  \perp}$	$15.106 - i 0.4844$

a good way to separate bulk and surface contributions for bulk terminated surfaces, although any such distinction has to be arbitrary<sup>6</sup>. It can be seen immediately from Fig. (3), that both components have an exponential decay. They also have about the same contribution in absolute value to the reflection. The second harmonic response of the bulk is caused by the second harmonic local fields and the linear polarisability of the bulk. *The only source of nonlinearity is the outermost dipole layer.* Since the linear induction term can never be eliminated, surface and bulk can have no independent second harmonic behaviour.

In this paper we have made a microscopic model calculation of the SSHG produced by a Si (100) surface. We have shown the possibility to fit the results to experimental data. Since there is no one to one correspondence between microscopic and macroscopic models, it is not possible to compare our results directly with those obtained by other authors<sup>17,18</sup>. Our major conclusions however do not depend on the particular Si (100) case given as an ex-

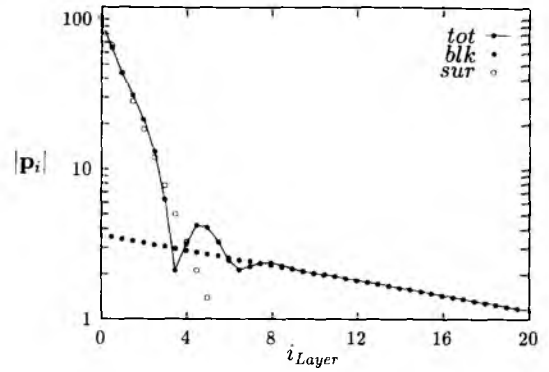


FIG. 3. Calculated nonlinear dipole strength  $|p_i|(2\omega)$  (in units of  $|\mathbf{E}_0|^2\beta_0$ ) as a function of layer-index for p-polarised excitation, ( $\theta = 45^\circ$ ,  $\Omega = 0^\circ$ ), total strength (total), normal mode part (bulk) and difference of those (surface)

ample. Purely microscopic models, as treated here, show clearly that linear and nonlinear responses, as a result of second harmonic local field effects, are tightly interwoven. Anisotropy showed this dependence, but we have intentionally assigned the nonlinearity to a single dipole layer, to demonstrate clearly the occurrence of second harmonic sources produced by a linear bulk. Phenomena going beyond the simple model description of this paper, will be subject of future work.

<sup>1</sup> D. Guidotti, D.A. Driscoll and H.J. Gerritsen, *Solid State Commun.* **46**, 337 (1983).

<sup>2</sup> J.A. Litwin, J.E. Sipe and H.M. van Driel, *Phys. Rev. B* **31**, 5543 (1985).

<sup>3</sup> H.W.K. Tom, T.F. Heinz and Y.R. Shen, *Phys. Rev. Lett.* **51**, 1983 (1983).

<sup>4</sup> C.W. van Hasselt, M.A. Verheijen and Th. Rasing, *Phys. Rev. B* **42**, 9263 (1990).

<sup>5</sup> N. Bloembergen, R.K. Chang, S.S. Jha and C.H. Lee, *Phys. Rev.* **174**, 813 (1968).

<sup>6</sup> J.E. Sipe, D.J. Moss and H.M. van Driel, *Phys. Rev. B* **35**, 1129 (1987).

<sup>7</sup> W.L. Schaich and B.S. Mendoza, *Phys. Rev. B* **45**, 14279 (1992).

<sup>8</sup> Peixian Ye and Y.R. Shen, *Phys. Rev. B* **28**, 4288 (1983).

<sup>9</sup> C.M.J. Wijers, Th. Rasing and R.W.J. Hollering, *Solid State Commun.* **85**, 233 (1993).

<sup>10</sup> C.M.J. Wijers and G.P.M. Poppe, *Phys. Rev. B* **46**, 7605 (1992).

<sup>11</sup> G.P.M. Poppe, C.M.J. Wijers and A. van Silfhout, *Phys. Rev. B* **44**, 1825 (1991).

<sup>12</sup> W.L. Mochán and R.G. Barrera, *Phys. Rev. Lett.* **55**, 1192 (1985).

<sup>13</sup> D.E. Aspnes and A.A. Studna, *Phys. Rev. B* **27**, 985 (1983).

<sup>14</sup> P. Guyot-Sionnest, W. Chen and Y.R. Shen, *Phys. Rev. B* **33**, 8254 (1986).

<sup>15</sup> H.W.K. Tom, Ph. D. Dissertation, University of California, Berkeley (1984).

<sup>16</sup> H. Wormeester, D.J. Wentink, P.L. de Boeij, C.M.J. Wijers and A. van Silfhout, *Phys. Rev. B* **47**, 12663 (1993).

<sup>17</sup> J.I. Dadap, B. Doris, Q. Deng, M.C. Downer, J.K. Lowell and A.C. Diebold, *Appl. Phys. Lett.* **64**, 2139 (1994).

<sup>18</sup> G. Lüpke, D.J. Bottomley and H. M. van Driel, *Phys. Rev. B* **47**, 10389 (1993)